CHAPTER 3

Thermo-kinetic analysis, thermodynamic parameters and comprehensive pyrolysis index of *Melia azedarach* sawdust as a genesis of bioenergy

Abstract

Energy demands are dynamic and intensifying demand of energy led to execute this study in order to analyze the thermal degradation characteristics of *Melia azedarach* sawdust (MAS) collected from sawmill intending to examine its pyrolytic performance for bioenergy and biofuel production. The inceptive characterizations which include proximate, ultimate, component analysis and higher heating value (HHV) were carried out so as to scrutinize its worth for pyrolysis. Furthermore, thermogravimetric (TG) experiments were performed in temperature hovering from ambient temperature to 900 ℃ at three different slow rates of heating (10, 20 and 30 ℃/min) under inert ambient condition. Findings of TG analysis revealed 210 to 480 ℃ as the maximum devolatilization temperature range during thermal degradation of MAS. Kinetic and thermodynamic parameters were estimated using three iso-conversional models i.e., Kissinger-Akahira-Sunose (KAS), Flynn-Wall-Ozawa (FWO) and Starink and average activation energy was found to be 161.18, 162.68 and 161.41 kJ/mol, respectively. The obtained values of Gibbs free energy (ΔG) were 185.98, 185.91and 185.97 kJ/mol and that of change in enthalpy (ΔH) were 155.91, 157.47 and 156.19 kJ/mol for KAS, FWO and Starink models, respectively. Master plot along with Criado method revealed a complex mechanism of the reaction. Average and maximum decomposition rates, as well as initial devolatilization and peak temperatures, shifted to higher values with an

increase in heating rate. Comprehensive pyrolysis index (CPI) exhibited higher value at higher heating rate which indicates the suitability of pyrolysis of MAS at a high heating rate. All these findings coupled with 16.34 MJ/kg HHV inferred the suitability of MAS for bioenergy generation as it exhibits remarkably high potential for bioenergy and biofuel generation. Thus, it can be a concrete step towards clean energy generation along with a balance between economy and ecology with desire to strengthen our energy self-sufficiency.

3.1 Introduction

Exploration of feedstocks that are novel and inexhaustible has become indispensable for attaining clean and perennial energy aspirations. With increase in the population and adaptation of high living standards by the people around the globe, the exigency of energy is surging swiftly. Conventional fossil-based sources of energy such as coal and petroleum products are non-renewable in nature and are present only in confined quantities. Apart from limited availability, these sources of energy are a profuse source of environmental pollution like air pollution, acid rain and greenhouse gas emission which is hazardous. So, the quest for alternative sources of energy which are renewable, green and sustainable is the need of the hour. It is high time that we should heed towards renewable sources of energy in order to plummet our reliability on conventional energy sources. Renewable sources of energy will help us combat all the limitations of non-renewable sources of energy because security of energy, access of energy for present and forthcoming generations, development in social as well as economical aspects, climatic change mitigation along with the reduction in adverse impacts on environment and ecology could be achieved by exploring renewable sources of energy (Owusu and Asumadu-Sarkodie, 2016). In present scenario, around 84% of energy demand is being attained by fossil-based fuels (Rapier R, 2020). Recently, an increase of 2.5% per annum

was recorded for the utilization of biomass in the form of fuel (Hussain et al., 2019; Shahid et al., 2019). Waste biomass-based feedstocks are a promising renewable source of energy as they are carbon neutral and have ultralow sulfur and nitrogen content. There are various routes by which biomass energy can be extracted for instance biological fermentation, direct combustion and thermochemical conversion (Wang et al., 2020). Pyrolysis is an efficient thermochemical transformation process performed in an inert atmosphere which yields products comprising of liquid bio-oil, solid bio-char and non-condensable pyrolytic gases. Bio-oil can be upgraded to petroleum fuel grade for use in engines, bio-char could be utilized as a potent and sustainable adsorbent for the purpose of wastewater treatment, soil remediation (Mukherjee et al., 2014), as meso-porous activated carbon precursor (Al-Layla et al., 2021), as carbon sequestration agent (Tarek et al., 2015), in fuel cells (Jinshuai et al., 2014) and supercapacitors (Rakesh et al., 2015). Bio-oil has high acidic and oxygen content along with high unsaturation degree and also it undergoes chemical reactions such as polymerization, condensation and oxidation upon storage which restrict its usage as a direct fuel. Thus, upgrading of bio-oil is required (Fadhil and Kareem, 2021). Pyrolytic gases which mainly comprise of syngas can be employed for industrial purposes.

Biomass feedstock includes agriculture crops and their residue, food processing waste, wood and sawdust, algae and aquatic plants. Wood sawdust is a major waste produced in the timber industry (Gupta and Mondal, 2018). On an average around 12-25 kg of sawdust is produced during processing of 100 kg of wood (Mahin, 1999). For disposal of sawdust, burning in open air, abandoning at sawmills, in landfills and water bodies are common practices. So, utilization of sawdust for bio-energy generation via pyrolysis will serve the dual purpose of energy generation and waste management simultaneously. Like other lignocellulosic biomass materials, wood sawdust also consists of three paramount

components which are cellulose, hemicellulose and lignin. Decomposition of these components take place in different temperature ranges (Altamer et al., 2021). The quantity and quality of pyrolysis products are influenced by the composition of biomass, reaction conditions like temperature, particle size, residence time and rate of heating (Wang et al., 2021). Bio-oil yield increases with increasing temperature up to certain range, residence time governs extent of biomass interaction in heating zone of the reactor, feedstock particle size controls heat and mass transfer and rate of heating influences product yield distribution of pyrolysis due to unique depolymerization and secondary thermal cracking reactions corresponding to distinct heating rates (Fadhil, 2020). Thus, a detailed study of biomass degradation is necessary before employing it for the production of bioenergy. It is not only essential for better product yield but also for designing and scale-up of pyrolysis plant.

Thermogravimetric analysis (TGA) is an efficient tool to examine the thermal degradation characteristics, kinetics and thermodynamics of biomass degradation (Yasmin et al., 2021). Modelling of biomass degradation is a quite tedious job when the material is exposed to a high-temperature environment owing to a composite nexus of combustion, fluid dynamics accompanied by heat and mass transfer, and kinetics. Biomass pyrolysis reaction kinetics is extremely complicated because of the generation of intermediate complexes. TGA is useful in determining the temperature at which pyrolysis should be carried out as it reveals cellulose, hemicellulose and lignin degradation temperature range. TGA facilitates the evaluation of kinetic triplets and thermodynamic parameters as a function of temperature and time. Using model-free methods combined with master plot is a quintessential approach (Alves et al., 2020). Model-free methods like Kissinger-Akahira-Sunose (KAS), Flynn-Wall- Ozawa (FWO) and Starink are used to evaluate activation energy (E) by plotting curves corresponding to different heating rates (β) and

conversion degree (α), further pre-exponential factor (*A*) and thermodynamic parameters which include change in enthalpy (Δ*H*), Gibbs free energy (Δ*G*), along with entropy (Δ*S*). Pyrolysis performance is characterized with the help of several pyrolysis performance parameters like maximum and average decomposition rates ($-R_p$ and $-R_a$), initial devolatisation and peak temperatures (T_i and T_p), temperature range of half-peak width ($\Delta T_{1/2}$) and comprehensive pyrolysis index (CPI). In the literature, pyrolysis kinetics has been reported for numerous biomass materials which include elephant grass, rice husk (Braga et al., 2020), agriculture straw and pinewood (Magdziarz et al., 2020), Indian sagwan sawdust (Gupta and Mondal, 2018), tobacco waste (Wu et al., 2015), red pepper waste (Maia and de Morais, 2016), para grass (Ahmad et al., 2017a) and acai seed (Alves et al., 2021).

Although, sawdust of many other kinds of wood have been explored for pyrolysis and comprehensive study of their kinetic and thermodynamic properties have been reported but comprehensive pyrolysis index, kinetics and thermodynamic study of *Melia azedarach* Sawdust (MAS) is reported for the very first time here in this paper. It is worth emphasizing that seeds of *Melia azedarach* have been used for pyrolysis but prior to this study no attempt has been made for utilization of its sawdust for biofuel and bioenergy generation using pyrolysis. *Melia azedarach* is a species that is a deciduous tree of the mahogany family, Meliaceae. It is known by many common names like pride of India, Persian lilac, syringa berrytree, Cape lilac, bead-tree, chinaberry tree, white cedar or Indian lilac. It is widely used for furniture due to its fungal resistant properties and is also used in logistic packaging and paper pulp as it grows rapidly. Large quantities of MAS are produced annually, that is a promising feedstock for pyrolysis. First of all, characteristic evaluation which included proximate, ultimate analysis and higher heating value determination was done. Next, this paper focused on determination

of thermal degradation characteristics by carrying out TGA at various heating rates (10, 20 and 30 °C/min) in an inert ambience. Kinetic predictions (activation energy and pre-exponential factor evaluation) were done by employing three model-free iso-conversional methods which included KAS, FWO and Starink models. Master plots were applied to gain the knowledge of governing reaction mechanism. Further, thermodynamic assessment like ΔH, ΔG and ΔS was done. Analysis of pyrolysis performance was done by evaluating CPI values at heating rates of 10, 20 and 30 °C/min. The data thus obtained inferred that MAS would prove to be an excellent biomass material for bioenergy generation.

3.2 Material and methods

3.2.1 Raw material

MAS which was used as the feedstock in this study was collected from a sawmill near IIT (BHU) Varanasi, India. First of all, it was quickly cleaned with normal tap water 4-5 times for removing the dirt and dust like non-native particles adhered to its external surfaces. This was immediately followed by washing with double distilled water so as to get rid of any grime or similar unwanted contaminants sticking to its surfaces. Then, it was perpetually kept in direct sunlight for 3 days followed by keeping it in the oven maintained at 105 °C until getting constant mass of the sample. Finally, it was sieved with -60 + 80 mesh to obtain the particles having the size in the range of 0.18–0.25 mm. These well-primed samples were then stored in sample containers and were kept in desiccators at room temperature for experimental purpose.

3.2.2 Analysis of physicochemical properties of MAS

Standard methods of ASTM were used for carrying out proximate analysis of MAS samples prepared after washing with double distilled water followed by sun drying and oven drying. Standard ASTM methods i.e., ASTM D3173, ASTM D3174 and ASTM

D3175 were used for the determination of the moisture content (MC), ash content (AC) and volatile matter (VM) present in the sample MAS. Fixed carbon content possessed by MAS was obtained by difference. Eq. (3.1) was used for calculating the fixed carbon (FC) content present in the sample.

$$FC = 100 - (VM + MC + AC) \quad (3.1)$$

Here, MC, VM, AC and FC are in wt.%.

An elemental analyzer (EURO EA, EUCO ECTOR instruments and software, Italy) was deployed to analyze the amount of carbon (C), hydrogen (H), nitrogen (N) and sulfur (S) content present in the sample. Eq. (3.2), as given below, was used for the purpose of calculation of amount of oxygen (O).

$$O = 100 - (C + H + N + S) \quad (3.2)$$

Here, C, H, N, S and O are in wt.%.

Van Soest standard protocols were followed for component analysis (hemicellulose, cellulose and lignin) of MAS (Gupta and Mondal, 2018). For estimation of higher heating value (HHV) of MAS, a bomb calorimeter (Rajdhani Scientific, NSTTS Co. New Delhi, India) was used.

3.2.3 Thermogravimetric experiments

A thermal analyzer (TGA 50, M/s Shimadzu (Asia Pacific) Pte Ltd.) was used for carrying out the TG experiments. Samples of MAS powder were kept in crucible made out of aluminium oxide and the temperature was raised from ambient to 900 ℃. Experiments were accomplished at three distinct rates of heating (10, 20 and 30 ℃/min) under non-isothermal conditions. Nitrogen gas of 99.99% purity was used as sweeping gas while performing experiments at a flow rate of 100 mL/min.

3.2.4 Kinetic analysis

The kinetic triplet, which consists of activation energy (E), frequency factor (A) and reaction mechanism (f(α)), is essential so as to provide an elaboration of the process from mathematical point of view. Given below reaction scheme is used to represent the thermochemical conversion of MAS.

$$A(biomass) \rightarrow B(biochar) + C(condensable\ and\ non - condensable\ gaseous\ products) \quad (3.3)$$

Under non-isothermal operating conditions, reduction of mass in MAS was registered as a function of temperature and for representation of rate of conversion (dα/dt) general kinetic model can be used as given by the following equation:

$$\frac{d\alpha}{dt} = k(T).f(\alpha) \quad (3.4)$$

where α represents degree of conversion of biomass, t stands for time (in seconds, s), T denotes the absolute temperature in Kelvin (K), $k(T)$ represents the rate of reaction which is dependent upon temperature and $f(\alpha)$ is a function of conversion which is temperature independent. In accordance with Arrhenius equation k can be articulated as follows:

$$k(T) = A\, e^{\frac{-E}{RT}} \quad (3.5)$$

where A denotes the frequency factor which is often called as pre-exponential factor (s^{-1}), E stands for the activation energy (J/mol), R stands for the universal gas constant (J/mol.K) and T represents the reaction temperature (K).

The following expression is used for conversion of biomass:

$$\alpha = \frac{W_i - W_t}{W_i - W_f} \quad (3.6)$$

Here, *Wi*, *Wt* and W_f stand for initial mass of sample (mg), mass of sample at time *t* (s) and final mass of the sample (mg) left as residue after reaction, respectively.

Since the rate constant, $k(T)$ is a function of temperature and can be expressed by using the Arrhenius law. Thus, by substituting k(T) from equation (3.5) into the equation (3.4), we get expression for $d\alpha/dt$ as:

$$\frac{d\alpha}{dt} = A\, e^{\frac{-E}{RT}} f(\alpha) \tag{3.7}$$

In the given study, at constant heating rate, β (°C/min) sample temperature was varied with respect to time and β can be expressed as follows:

$$\frac{dT}{dt} = \beta \tag{3.8}$$

On using equation (3.8) in equation (3.7), we get

$$\frac{\mathrm{d}\alpha}{\mathrm{dT}} = \left(\frac{A}{\beta}\right) \exp\left(-\frac{\mathrm{E}}{\mathrm{RT}}\right) . \mathrm{f}(\alpha) \tag{3.9}$$

On rearranging the above equation, we get expression as:

$$\frac{d\alpha}{f(\alpha)} = \frac{A}{\beta} \exp\left(-\frac{\mathrm{E}}{\mathrm{RT}}\right) . dT \tag{3.10}$$

In view of that the conversion of biomass can be expressed as a function of heating rate (β) and temperature, and on left hand and right-hand side integration of equation (3.10) furnishes given below equation:

$$\mathrm{G}(\alpha) = \int_0^{\alpha} \frac{d\alpha}{f(\alpha)} = \frac{A}{\beta} \int_0^{\mathrm{T}} \exp\left(-\frac{E}{RT}\right) dT \tag{3.11}$$

Here, $G(\alpha)$ is used for representing integral function of conversion and $f(\alpha)$ is used for representing an algebraic expression which describes the kinetic model for decomposition of matter in solid-state. For the case of non-isothermal thermogravimetric analysis kinetic parameters can be analyzed by making use of two approaches namely free-model and fitting-model approach. For model-free methods assumption of any kind of reaction kinetics is not a pre-requisite whereas for model-fitting a prompt model is required in which data is fit. Meanwhile, iso-conversional models are independent of any reaction

model and thus only TG data are required at various heating rates as rate of reaction is dependent only on temperature. The kinetic parameters are reaped as a function of temperature or conversion.

Iso-conversional methods prove to be an eminent tool to explain a tedious process in which complex multi-step chemical reactions occur in a spree. These iso-conversional models are defined by either integral or differential methods.

3.2.4.1 Kissinger-Akahira-Sunose Method

Kissinger-Akahira-Sunose (Kissinger, 1957; Akahira and Sunose, 1971) proposed an integral iso-conversional method which was based on the following equation:

$$\ln\left(\frac{\beta}{T^2}\right) = \ln\left(\frac{A_0 E}{RG(\alpha)}\right) - \frac{E}{RT_\alpha} \quad (3.12)$$

At a particular conversion value (α), the plot $\ln\frac{\beta}{T^2}$ vs $\frac{1}{T_\alpha}$ which is obtained with the help of thermograms produced at different heating rates (10, 20 and 30 °C/min), gives a straight line and its slope is used to calculate activation energy.

3.2.4.2 Flynn–Wall–Ozawa method

Ozawa Flynn Wall method (Ozawa, 1965; Flynn and Wall, 1966) is an integral method which helps in calculation of activation energy. For this method linear Doyle's approximation (Doyle, 1965; Galwey and Brown 1999) for estimation of temperature's integral was used. The equation of this model is as follows:

$$\ln(\beta) = \ln\left(\frac{A_0 E}{RG(\alpha)}\right) - 5.331 - 1.052\left(\frac{E}{RT_\alpha}\right) \quad (3.13)$$

At specified value of conversion $\ln(\beta)$ vs $\frac{1}{T_\alpha}$ was plotted and the slope ($-1.052\frac{E}{R}$) of the straight line thus obtained was used to calculate value of activation energy.

3.2.4.3 Starink method

Starink (Starink, 1996) analyzed the methods of KAS and FWO and on combining both

these methods, equation obtained was as follows:

$$\ln\left(\frac{\beta}{T^{1.92}}\right) = constant - 1.0008\left(\frac{E}{RT_\alpha}\right) \quad (3.14)$$

For different conversion values at three different constant heating rates, plots of $\ln\left(\frac{\beta}{T^{1.92}}\right)$ vs. $\frac{1}{T_\alpha}$ were drawn and the straight line thus obtained has a slope of $\frac{-1.0008E}{R}$ which was used to evaluate the value of activation energy.

3.2.5 Determination of reaction model

Determination of reaction model is an integral part of kinetic study. Master plots remain unaffected by kinetic parameters such as activation energy values and pre-exponential factor (Luo, 2021). International Confederation of Thermal Analysis and Calorimetry (ICTAC) recommends use of method of Z-master plot for identifying reaction model by employing an ideal set of various models (Pérez-Maqueda, 2011). By combination of integral and differential forms of reaction mechanism and Z-master plot thus obtained can be written as follows:

$$Z(\alpha) = f(\alpha).G(\alpha) = \left(\frac{d\alpha}{dt}\right) T^2 \left[\frac{\pi\left(-\frac{E}{RT}\right)}{\beta T}\right] \quad (3.15)$$

The function shape is independent of the term $\left[\frac{\pi\left(-\frac{E}{RT}\right)}{\beta T}\right]$ (Galwey and Brown, 1999; Pérez-Maqueda et al., 2011), in normalize form eq. (3.15) can be written as:

$$\frac{Z(\alpha)}{Z(0.5)} = \frac{f(\alpha) \times g(\alpha)}{f(0.5) \times g(0.5)} = \left(\frac{T_\alpha}{T_{0.5}}\right)^2 \times \left(\frac{\left(\frac{d\alpha}{dt}\right)_\alpha}{\left(\frac{d\alpha}{dt}\right)_{0.5}}\right) \quad (3.16)$$

For thermally decomposed MAS, reaction model which is also known as reaction mechanism was estimated using Z-master plot specified by Criado method as stated above in eq. 3.16. The term $\frac{f(\alpha)\times g(\alpha)}{f(0.5)\times g(0.5)}$ is evaluated for several ideal kinetic models of differential and integral patterns observed for solid state reactions as presented in Table

3.1. This calculation imparts various theoretical profiles and the term $\left(\frac{T_\alpha}{T_{0.5}}\right)^2 \times \left(\frac{\left(\frac{d\alpha}{dt}\right)_\alpha}{\left(\frac{d\alpha}{dt}\right)_{0.5}}\right)$ is determined at a specific heating rate by using values obtained from experiment and thus providing us with a single plot.

The plot which is obtained by using above expression is called as master plot. This plot needs no information about any kinetic parameter such as frequency factor or activation energy etc.The temperature at a specific conversion α is denoted by T_α, for example at 50% conversion the temperature is denoted by writing $T_{0.5}$. The conversion value α = 0.5 was chosen as point of reference because for all the experimental and theoretical curves $\frac{Z(\alpha)}{Z(0.5)}$ term consolidates to unity. In this manner, the theoretical and experimental plots were compared and the best fit model was determined for the identification of reaction's kinetic features (Pérez-Maqueda et al., 2019; Mishra et al., 2015; Singh et al., 2020).

Table 3.1. Expressions of f(α) and g(α) for some reaction mechanisms occurring in solid state

Mechanism	**Model**	**Differential form f(a)**	**Integral form g(a)**
Nucleation models			
P2/3	Power law	$(2/3)\alpha^{-1/2}$	$\alpha^{3/2}$
P2	Power law	$2\alpha^{1/2}$	$\alpha^{1/2}$
P3	Power law	$3\alpha^{2/3}$	$\alpha^{1/3}$
P4	Power law	$4\alpha^{3/4}$	$\alpha^{1/4}$
Sigmoidal rate eq.			
A1	Avarami–Erofeev	$1/2(1-\alpha)[-\ln(1-\alpha)]^{1/3}$	$[-\ln(1-\alpha)]^{2/3}$
A2	Avarami–Erofeev	$2(1-\alpha)[-\ln(1-\alpha)]^{1/2}$	$[-\ln(1-\alpha)]^{1/2}$
A3	Avarami–Erofeev	$3(1-\alpha)[-\ln(1-\alpha)]^{2/3}$	$[-\ln(1-\alpha)]^{1/3}$

A4	Avarami–Erofeev	$4(1-\alpha)[-\ln(1-\alpha)]^{3/4}$	$[-\ln(1-\alpha)]^{1/4}$
F2	Contracting cylinder	$2(1-\alpha)^{1/3}$	$1-(1-\alpha)^{1/2}$
F3	Contracting sphere	$(1-\alpha)^{2/3}$	$1-(1-\alpha)^{1/3}$
Diffusion models			
D1	1D diffusion	$1/(2\alpha)$	α^2
D2	2D diffusion (Valensi)	$[-\ln(1-\alpha)]^{-1}$	$(1-\alpha)\ln(1-\alpha)]+\alpha$
D3	3D diffusion (Jander)	$3/2(1-\alpha)^{2/3}[1-(1-\alpha)^{1/3}]^{-1}$	$[1-(1-\alpha)^{1/3}]^2$
D4	3D diffusion (Ginstling)	$3/2[(1-\alpha)^{1/3}-1]^{-1}$	$1-2/3\alpha-(1-\alpha)^{2/3}$
Reaction order models			
R1	First order	$1-\alpha$	$-\ln(1-\alpha)$
R2	Second order	$(1-\alpha)^2$	$(1-\alpha)^{-1}-1$
R3	Third order	$(1-\alpha)^3$	$1/2[(1-\alpha)^{-2}-1]$

3.2.6 Thermodynamic assessment

Once activation energy was determined then calculation of pre-exponential factor (A) (s^{-1}) was done at different conversion values. Thereafter, the thermodynamic parameters, like change of enthalpy (ΔH) (kJ/mol), Gibbs free energy (ΔG) (kJ/mol), and entropy (ΔS) (J/mol.K) for the transition states were evaluated using the following equations:

$$A = \frac{\beta \times E \times exp\left(\frac{E}{R \times T_p}\right)}{R \times T_p^2} \quad (3.17)$$

$$\Delta H = E - R \times T\alpha \quad (3.18)$$

$$\Delta G = E + R \times Tp \times ln\left[\frac{K_B \times T_p}{h \times A_0}\right] \quad (3.19)$$

$$\Delta S = (\Delta H - \Delta G)/Tp \quad (3.20)$$

Where, T_p stands for the peak temperature value (in K) obtained from DTG plot at a specific heating rate, K_B and h, are for the Boltzmann constant having a value of

1.381×10^{-23} J/K and the Planck's constant having a value of 6.626×10^{-34} J.s, respectively.

3.2.7 Analysis of pyrolysis performance

Comprehensive pyrolysis index (CPI) was evaluated to quantify pyrolysis performance as follows:

$$CPI = \frac{(-R_p)(-R_a)(M_f)}{(T_p)(T_i)(\Delta T_{1/2})} \tag{3.21}$$

Where, $-R_p$ and $-R_a$ are maximum and average decomposition rates respectively, M_f stands for weight loss (wt.%), T_p represents peak temperature (°C), T_i is initial devolatisation temperature (°C) and $\Delta T_{1/2}$ is temperature range of half-peak width (when R/R_p =1/2) (°C). Higher values of CPI indicate better pyrolysis performance.

3.3 Results and discussion

3.3.1 Physicochemical properties of MAS

The heating value of biomass is extremely affected by volatile content, the content of the ash, and also by the elemental composition of hydrogen, carbon and oxygen. Proximate analysis was carried out in order to figure out MC, VM, AC and FC content present in the MAS sample. Table 3.2 shows all these contents in a tabulated fashion along with the same data for other biomass materials reported in literature.

The result of proximate analysis showed that MAS possesses low MC, low AC and high VM. When moisture content is less than 10 wt.% then it leads to a high rate of heat transfer in pyrolysis process (Reed, 1981) and in MAS sample moisture content was 6.64 wt.%. MAS samples prepared after cleaning with double distilled water, sun drying, oven drying followed by size reduction were used for proximate and ultimate analysis. Biomass which has high volatile matter content is desirable for the purpose of production of bio-oil because it can easily be devolatized as compared to low volatile

matter containing material (Nanda et al., 2014). MAS biomass was composed of 78.30 wt.% volatile matter. All these properties make it a suitable candidate for using in thermochemical conversion process for generating biofuel. The proportion of content of moisture, volatile matter content, ash content and content of fixed-carbon existing in the MAS are in the range of lignocellulosic biomass (Nanda et al., 2014; Doshi et al., 2014).

Table 3.2. Proximate analysis of MAS (wt.%)

Property	**MAS (present study)**	**Teak (Gupta et al., 2019)**	***Acacia nilotica* (Singh et al., 2020)**	**Pine sawdust (Mishra and Mohanty, 2018)**	**Sal sawdust (Asadullah et al., 2007)**
moisture content	6.64	3.87	6.46	5.90	8.88
volatile matter	78.30	78.17	79.08	77.80	76.03
ash content	2.04	3.53	0.78	0.79	1.14
fixed carbon* (by difference)	13.02	14.43	13.68	15.55	14.09

To know the elemental composition of carbon, hydrogen, nitrogen, oxygen and sulfur present in the MAS, ultimate analysis was performed. The results of the ultimate analysis and HHV of MAS and some other sawdust is presented in Table 3.3.

The results of the ultimate analysis of the biomass revealed that carbon, hydrogen, nitrogen and oxygen present in MAS were 43.84, 6.49, 0.88 and 48.79 wt.%, respectively. Sulfur content was far below the range of detection. The energy content present in biomass is severely influenced by its chemical or elemental (carbon, oxygen and hydrogen) composition and is adversely affected by the presence of moisture and

inorganic elements. Due to the presence of nitrogen and sulfur emission of NO_x and SO_x, respectively occurs which intensifies greenhouse gas effects. Since low nitrogen and negligible sulfur content was found to be present in MAS biomass which assures it is a potent material for biofuel generation in an eco-friendly manner. Component analysis of MAS revealed that it has 18.52 wt.% hemicellulose, 50.37 wt.% cellulose and 21.64 wt.% lignin. HHV indicates the amount of energy which can be extracted from biomass via combustion and for MAS it was 16.34 MJ/kg.

Table 3.3. Ultimate analysis of MAS (wt.%)

Element/ Property	MAS (present study)	Teak (Gupta et al., 2019)	*Acacia nilotica* (Singh et al., 2020)	Pine sawdust (Mishra and Mohanty, 2018)	Sal sawdust (Asadullah et al., 2007)
Carbon	43.84	49.17	43.69	46.82	49.83
Hydrogen	6.49	5.93	7.54	6.04	6.01
Nitrogen	0.88	1.03	0.47	0.14	0.58
Oxygen* (by difference)	48.79	43.87	48.30	46.98	43.56
H/C	1.59	1.44	0.17	0.13	1.45
O/C	0.75	0.70	1.10	1	0.66
HHV (MJ/kg)	16.34	17.73	18.66	18.59	18.20

3.3.2 Thermogravimetric analysis

TG curve depicts profile of mass loss as a function of temperature and DTG curve shows differential mass loss as a function of temperature (Doshi et al., 2014). Thermal behavior of MAS was recorded by performing thermogravimetric analysis experiments at

three different rates of heating 10, 20 and 30 ℃/min. The temperature in the range of ambient to 900 ℃ was used and 100 mL/min continuous purging rate was employed for nitrogen gas. As per the findings of previously work done in this field, degradation of biomass can be classified into several stages like water devolatilization, followed by decomposition of hemicellulose, cellulose and lignin decomposition (Font et al., 2005). Decomposition of hemicellulose mainly occurs in 220-315 ℃ temperature range. While major portion of cellulose degradation takes place in the range of 315-400 ℃ (Gašparoviè, 2012). Thermal decomposition of lignin takes place in a wide temperature range varying from 180 to 900 ℃ (Misse et al., 2018; Yang et al., 2007). The complete procedure of degradation of biomass can be classified into three different zones namely drying, devolatilization, and charring. Here drying zone or first zone is an indicator of moisture removal, meanwhile, hemicellulose and cellulose get thermally degraded in second zone and third zone shows the degradation of lignin.

In Fig. 3.1, 3.2 and 3.3 TG and DTG plots secured for various rates of heating (10, 20 and 30 ℃/min) are shown and these curves are used to describe the thermal decomposition profile of biomass. From TG curve that was drawn for heating rate of 10 ℃/min, it was observed that approximately 6% loss in mass took place in the temperature ranging from ambient to 115 ℃. This loss in mass is because of removal of moisture, few very volatile compounds and minerals' decomposition (Fan et al., 2022), which were existing in the biomass and thus it is a stage of release of moisture. Then TG curve plateaued up to 210 ℃. The next stage is the stage of release of volatiles and it is considered as the stage of utmost importance as on an average nearly 62% loss of mass was recorded in it. This stage of devolatilization varied from a temperature range of 210 to 480 ℃. Volatile release in MAS took place largely after temperature reached 270 ℃.

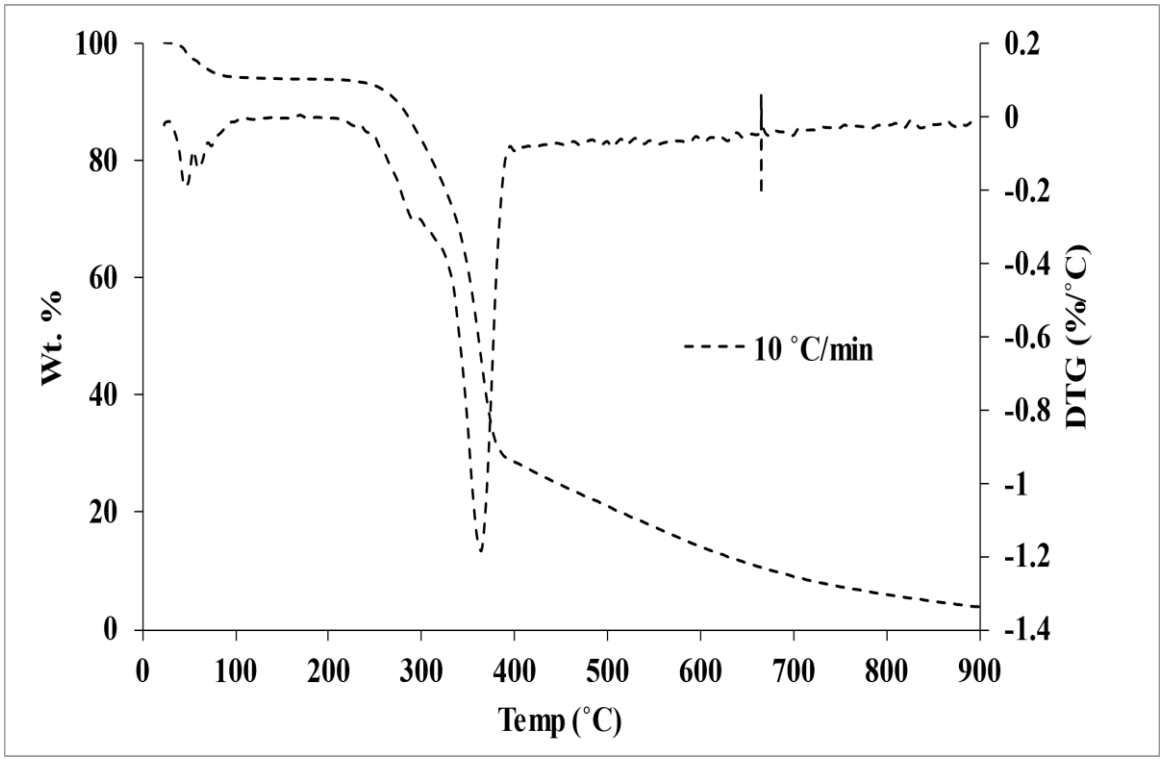

Figure 3.1. TG/DTG curve for 10℃/min heating rate

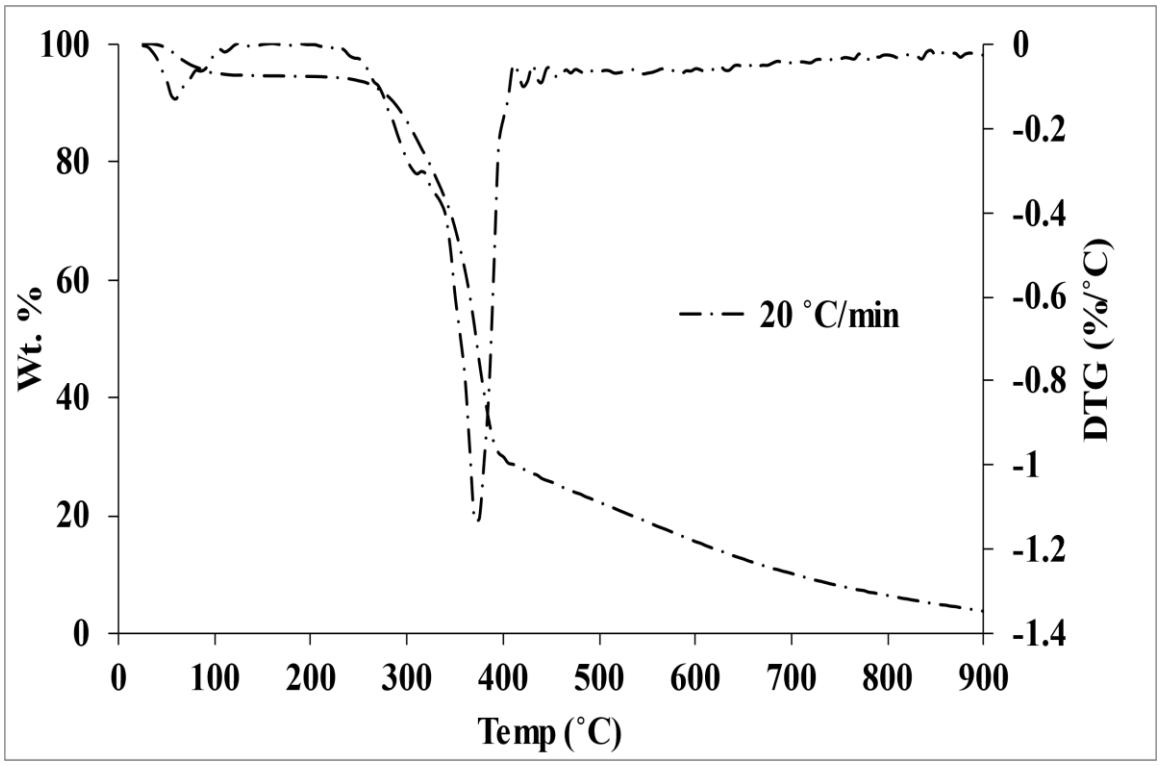

Figure 3.2. TG/DTG curve for 20℃/min heating rate

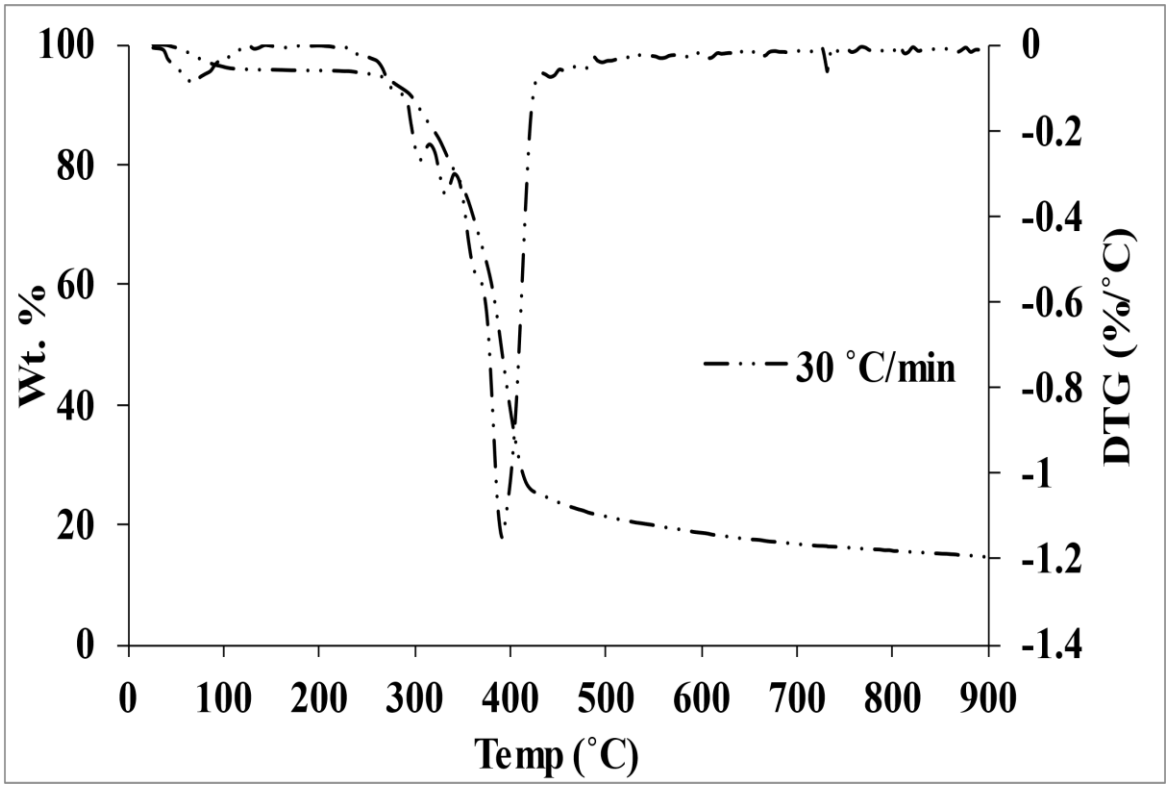

Figure 3.3. TG/DTG curve for 30℃/min heating rate

This second stage is called as active pyrolysis zone and is responsible for decomposition of hemicellulose and cellulose present in MAS. Decomposition of lignin happens over a very wide range of temperature starting from 180 ℃ and stretching till 900 ℃ and it happens in such a manner because of complexities arising due to polymorphism and non-occurrence of any fundamental structure (Khan et al., 2016). Decomposition of lignin takes place comparatively at much slower rate (Knoetze et al., 2010). Only a very little reduction in mass was observed beyond 600 ℃.

The temperature corresponding to which maximum loss in the mass was recorded is indicated by the positions of the peaks in DTG profiles as shown in Fig. 3.1, 3.2 and 3.3. Temperature at which maximum mass loss occurred was 364.63 ℃ corresponding to 10 ℃/min heating rate. And it jumped to 371.19 ℃ for 20 ℃/min and further shifted to 392.87 ℃ at 30 ℃/min heating rate.

Although, the temperature corresponding to maximum loss of mass elevated with elevation in heating rate from 10 to 20 and to 30 °C/min. The nature of shape of mass loss profiles did not alter with increase in rate of heating as per Figs. 3.1, 3.2 and 3.3. Only mass loss peak switched to a higher value of temperature with rise in rate of heating. This implied that mass loss was independent of whatever heating rate was applied. And the same is in agreement with the nature displayed by TG curves at various heating rates. This lateral movement to a higher temperature for degradation emphasizes the diversification in heat transfer to biomass depending upon variation of heating rate. Temperature differences and its gradient increase at low heat transfer rate giving rise to thermal lag between the outermost layer and inner parts of biomass.

3.3.3 Kinetic studies

An elaborated kinetic assessment is needed in order to figure out numerous kinetic and thermodynamic parameters. Since entire process of pyrolysis is comprised of multi-step reaction mechanism along with heterogeneous and complex reactions. Moreover, pyrolysis process exhibits reaction mechanism which is either seldom known or highly complex to be characterized with the help of ordinary kinetic models.

Iso-conversion model methodology is a way that makes it possible to carry out kinetic studies without pre-requisite knowledge of reaction mechanism (Šimon, 2004). The ICTAC advocates using iso-conversional methods for non-isothermal studies (Vyazovkin et al., 2011).

Results obtained by TG/DTG analysis were employed to evaluate the kinetic parameters for thermal degradation of MAS. In iso-conversional models it is assumed that reaction/phase conversion mechanism remains strictly unaltered with the change in rate of heating employed for carrying out the reaction.

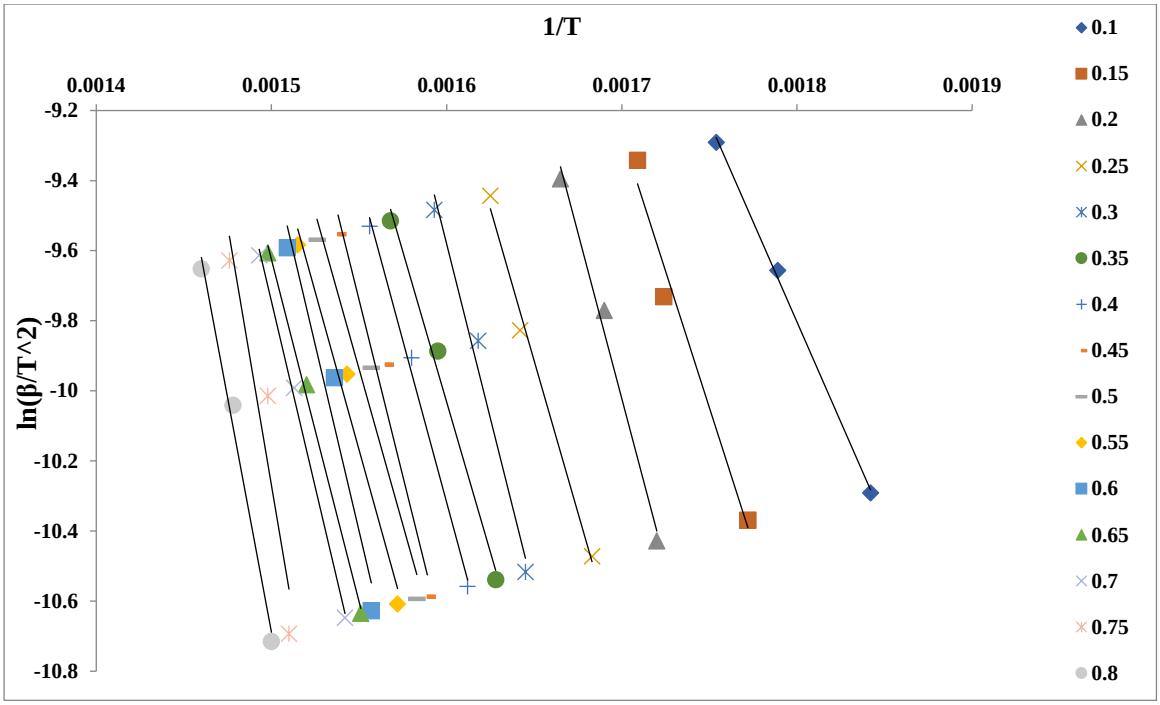

Figure 3.4. KAS integral model for activation energy calculation

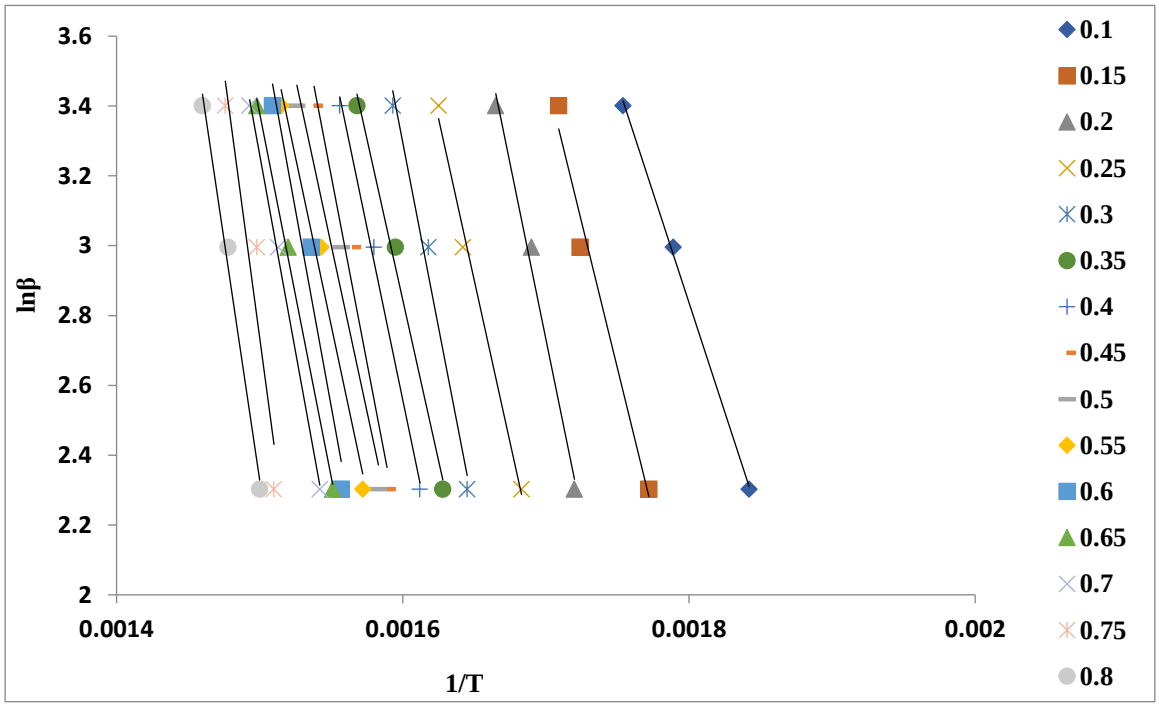

Figure 3.5. FWO integral model for activation energy calculation

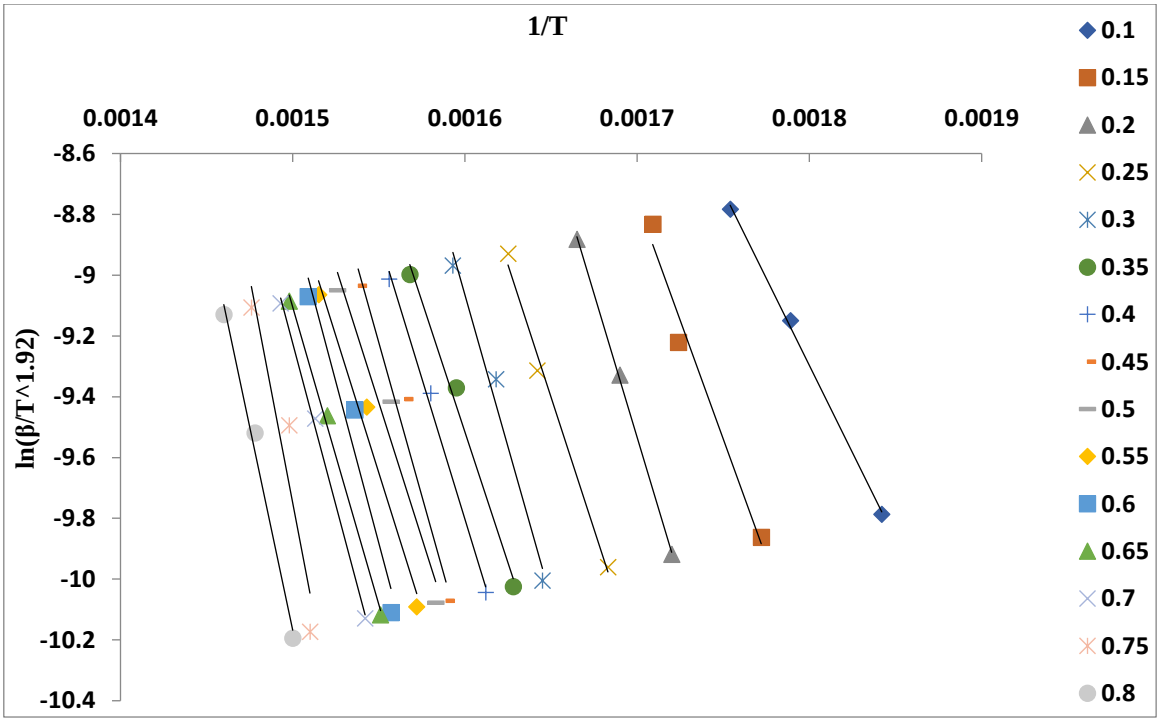

Figure 3.6. Starink integral model for activation energy calculation

In the present work three iso-conversional models applied were KAS, FWO and Starink. The profiles obtained for these prior mentioned models are illustrated in Figs. 3.4, 3.5 and 3.6. These three models were used to inspect the thermal decomposition kinetics involved in degradation of MAS for conversion ranging from 10 to 80% accompanied by a hike of 5% in a step wise manner to arrive at an apt result. The conversion data obtained for less than 10 and more than 80% were not used in the calculations in order to diminish the consequences of moisture and ash content.

In all the three above-mentioned methods, the activation energy was computed using the slope of trendlines obtained for various conversions as illustrated in Table 3.4. Satisfactory fitting of models was ensured owing to the fact that regression coefficient (R^2) figures ranged from 0.939 to 0.999. The average value of activation energy of MAS obtained from KAS, FWO and Starink iso-conversional model methods was found to be

Table 3.4. Activation energy at different mass conversions for different iso-conversional kinetic models

Conversion, α, %	KAS E, kJ/mol	R^2	FWO E, kJ/mol	R^2	Starink E, kJ/mol	R^2
10	94.92	0.999	99.04	0.999	95.20	0.999
15	129.47	0.976	132.04	0.979	129.74	0.977
20	157.10	0.989	158.67	0.991	156.73	0.999
25	144.30	0.992	146.72	0.993	144.58	0.992
30	165.76	0.981	167.44	0.984	166.04	0.982
35	142.68	0.990	145.48	0.992	142.98	0.990
40	153.53	0.995	155.91	0.995	153.82	0.995
45	167.44	0.962	169.17	0.967	167.72	0.962
50	147.91	0.955	150.76	0.960	148.21	0.955
55	149.66	0.978	152.53	0.981	149.97	0.978
60	176.39	0.946	177.98	0.952	176.68	0.946
65	162.29	0.997	164.66	0.997	162.60	0.997
70	176.35	0.998	178.03	0.998	176.63	0.998
75	227.68	0.939	223.47	0.943	227.79	0.939
80	222.27	0.991	218.22	0.991	222.37	0.991
Mean	**161.18**		**162.68**		**161.41**	

161.18, 162.68 and 161.41 kJ/mol respectively. Values of activation energy obtained showed a close agreement with that of many other biomass materials as reported by numerous authors in literature of their respective studies and are provided in Table 3.5. From Table 3.5 it is clear that activation energy for present study is less than that of most of the biomass materials listed, it clearly indicated the feasibility of MAS to be used for the generation of biofuels through pyrolysis process as low activation energy means it decomposes thermally at low temperature along with minimum energy demand. The trend followed by all the plots of iso-conversional models was similar and thus making this method acceptable for the purpose of calculation of activation energy.

Table 3.5. Comparison of activation energy obtained by various iso-conversional models for different biomass materials

Biomass	Sweeping gas flow rate (mL/min)	Heating rate (°C/min)	Model name	Mean E (kJ/mol)	References
Dahlia flower	N_2, 40	5, 10, 20	KAS FWO	220.12 229.81	(Mishra et al., 2020)
Maple leaf waste	N_2, 60	10, 20, 30, 40	FWO KAS	91.50 75.83	(Ahmad et al., 2021)
Accacia Nilotica	N_2, 20	5, 10, 15	KAS FWO Starink	211.49 221.58 211.89	(Singh et al.,2020)
Maize cob	N_2, 60	5, 10, 20	FWO KAS Starink	186.06 185.39 185.80	(Gupta and Mondal, 2019b)
Deodar sawdust	N_2, 200	10, 25, 50, 100	FWO KAS	180.60 179.20	(Rasool et al., 2018)
Pine sawdust	N_2, 50	5, 10, 15, 20, 25	KAS OFW	171.66 179.29	(Mishra and Mohanty, 2018)
Sal sawdust	N_2, 50	5, 10, 15, 20, 25	KAS OFW	148.44 156.58	(Mishra and Mohanty, 2018)
Arachis hypogaea shells	N_2, 100	10, 15, 25	KAS FWO Starink	173.65 173.5 171.83	(Dave et al., 2021)
Poplar wood	N_2	2, 5, 10, 15	KAS FWO	157.30 158.69	(Slopiecka et al., 2012)
MAS	N_2, 100	10, 20, 30	KAS FWO Staring	161.18 162.68 161.41	Present study

For all the three iso-conversional models activation energy against conversion profile depicted alike nature as observed from Fig. 3.7. Up to 20% conversion there was an increment in activation energy then slight plunging in its values occurred till 25%. After 30% decrease-increase pattern in activation energy was shown and plateauing nature of curve was observed from 50 to 55% conversion. After that activation energy increased with minute decrease corresponding to some conversion values. Increase in activation energy in later stages could be attributed to degradation of more lignin and less cellulosic component. This zig-zag increase decrease in activation energy with increasing conversion manifests the fact that degradation of biomass material is a complex and multi-step process incorporating a large number of chemical reactions occurring in parallel and series manner simultaneously.

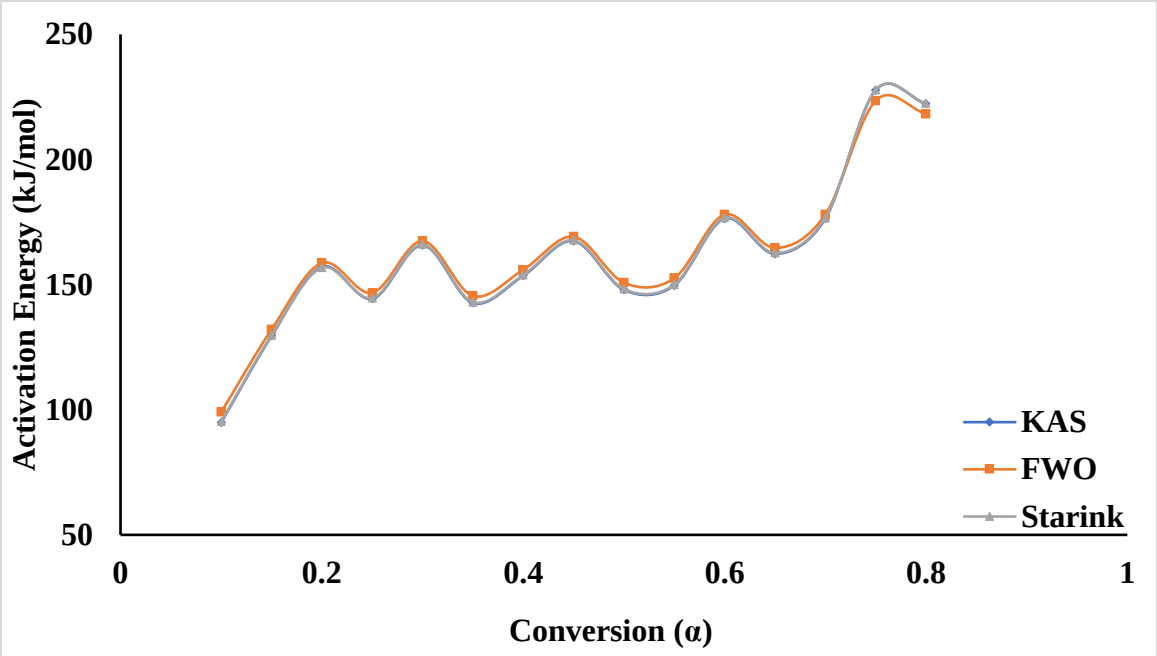

Figure 3.7. Activation energy as a function of conversion for different iso-conversional models

3.3.4 Determination of the reaction mechanism by using the master-plot

The $Z(\alpha)/Z(0.5)$ versus α (conversion) curves obtained at 10 ℃/min by employing various mechanism models as listed in Table 3.1 are shown in Fig. 3.8. In conversion range varying from 0.1 to 0.8, that means from 10 to 80% conversion the experimental and theoretical curve profiles were drawn using eq. 3.16 and reaction models described in Table 3.1, respectively. A close estimation of decomposition reaction mechanism is done by comparison of various theoretical plots with plot obtained for experimental values. From Fig. 3.8, it was observed that up to 20% conversion experimental curve showed nature similar to that of D2, D3, P4, and R1, thus it can be inferred that thermal degradation of MAS is governed by D2, D3, P4 and R1 mechanisms, where degradation occurs by diffusion, nucleation power law and second-order reaction model. These findings are in accordance with findings for eucalyptus clone pyrolysis (Doddapaneni et al., 2016) and sugarcane bagasse pyrolysis (Nam et al., 2019) where pyrolysis of biomass was governed by diffusion models during initial conversion. From 30 to 50% conversion range experimental curve followed trends similar to that of F3 and R1 which is an indicator of contracting cylinder and first-order random nucleation containing single nucleus on individual particle. As conversion proceeded to the range of 55 to 80 %, experimental curve well matched with F3, R1, R2 and R3 mechanism which pointed out that random nucleation models and contracting cylinder models are being followed. Beyond 80% conversion, it became tedious to identify any suitable model, which could be because of complex char decomposition. Above results are in harmonious agreement with the findings of many other studies done in this field (Mishra et al., 2015; Junges et al., 2002; Zheng et al., 2019).

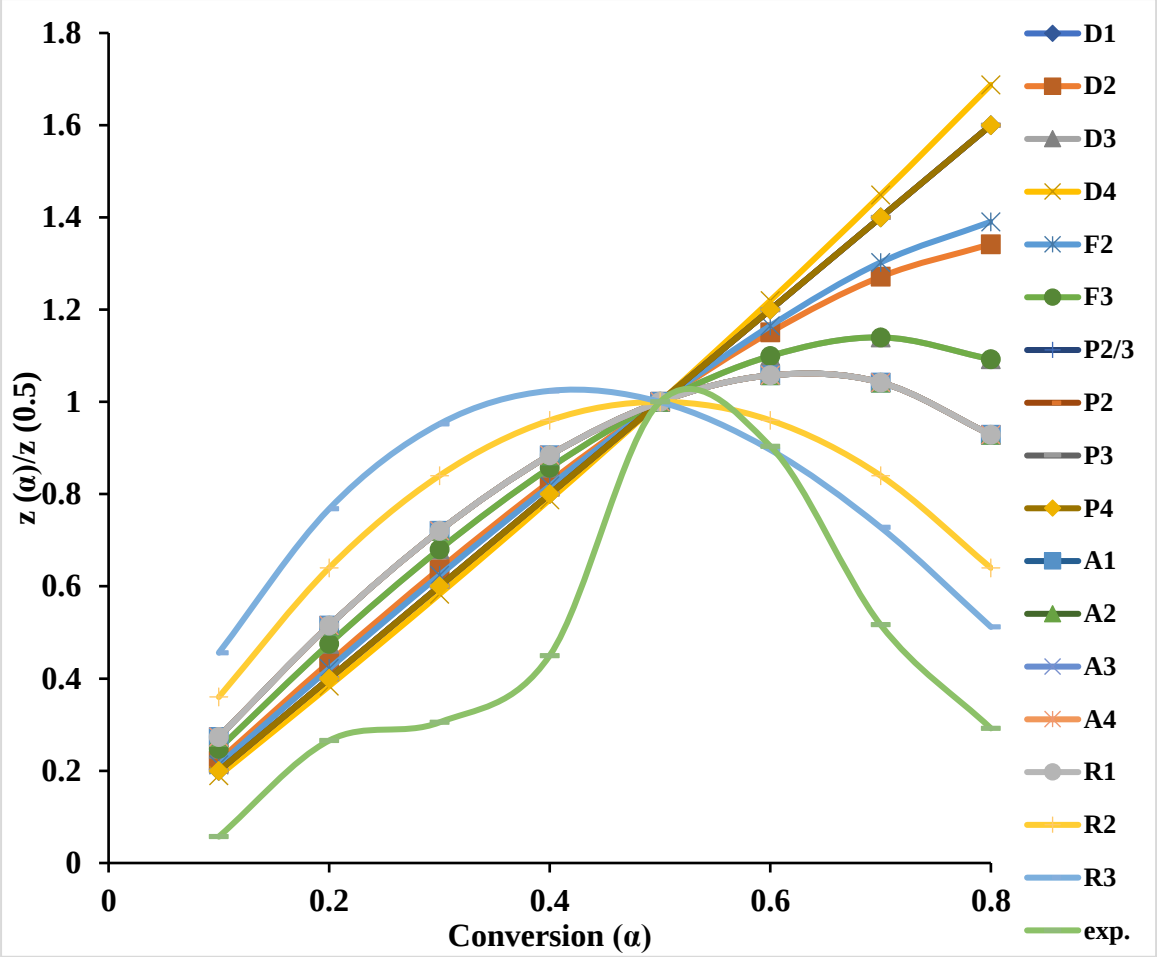

Figure 3.8. Master plots and experimental plots at 10 °C/min obtained by using the Criado method

3.3.5 Thermodynamic assessment

In addition to kinetic parameters, thermodynamic parameters also play a pivotal role for designing and scaling up of a proto type to commercial level successful plant of pyrolysis. These thermodynamic parameters provide us with basic knowledge regarding requirement of energy, thermodynamic equilibrium, feasibility of process and energy barrier while carrying out pyrolysis process. Apparent activation energy calculated in prior section by using different iso- conversional methods namely KAS, FWO and Starink corresponding to heating rate of 10 °C/min, were used for the purpose of determining thermodynamic parameters. In order to diminish the consequences arising

due to interaction amongst elements during thermal decomposition process, the lowest heating rate (10 ℃/min) was selected for thermodynamic parameter calculations (Yuan et al., 2017; Cao et al., 2014). Pre-exponential factor (A), change of enthalpy (ΔH), Gibbs free energy (ΔG), and entropy (ΔS) were calculated using eqs. 3.17, 3.18, 3.19 and 3.20, respectively. Results obtained for these calculations are presented in Table 3.6.

Table 3.6. Thermodynamic Parameters along with pre-exponential factor for different models

α (%)	A (s^{-1})	ΔH (kJ/mol)	ΔG (kJ/mol)	ΔS (J/mol.K)
KAS				
10	2.78×10^{05}	90.35	188.68	-154.18
15	2.56×10^{08}	124.72	187.03	-97.71
20	5.70×10^{10}	152.15	186.01	-53.08
25	4.69×10^{09}	139.31	186.46	-73.93
30	3.08×10^{11}	160.65	185.72	-39.31
35	3.42×10^{09}	137.52	186.52	-76.83
40	2.84×10^{10}	148.31	186.13	-59.29
45	4.27×10^{11}	162.14	185.67	-36.89
50	9.48×10^{09}	142.59	186.33	-68.57
55	1.34×10^{10}	144.31	186.27	-65.79
60	2.43×10^{12}	170.99	185.39	-22.59
65	1.57×10^{11}	156.87	185.84	-45.41
70	2.41×10^{12}	170.89	185.39	-22.74
75	4.99×10^{16}	221.93	184.04	59.41
80	1.75×10^{16}	215.95	184.17	49.83
Average		**155.91**	**185.98**	**-47.14**
FWO				
10	6.31×10^{05}	94.53	188.45	-147.27
15	4.25×10^{08}	127.35	186.93	-93.42
20	7.75×10^{10}	153.79	185.96	-50.44
25	7.53×10^{09}	141.79	186.37	-69.90
30	4.28×10^{11}	162.39	185.67	-36.49
35	5.91×10^{09}	140.38	186.42	-72.18
40	4.52×10^{10}	150.75	186.05	-55.34
45	5.98×10^{11}	163.94	185.62	-33.99
50	1.66×10^{10}	145.52	186.23	-63.83
55	2.34×10^{10}	147.25	186.16	-61.02
60	3.32×10^{12}	172.65	185.35	-19.91
65	2.49×10^{11}	159.31	185.75	-41.47
70	3.35×10^{12}	172.64	185.35	-19.92
75	2.21×10^{16}	217.79	184.14	52.76
80	8.04×10^{15}	211.98	184.27	43.46

Average		**157.47**	**185.91**	**-44.59**
Starink				
10	2.94×10^{05}	90.69	188.66	-153.62
15	2.71×10^{08}	125.05	187.02	-97.17
20	5.31×10^{10}	151.84	186.02	-53.59
25	4.96×10^{09}	139.65	186.45	-73.38
30	3.26×10^{11}	160.99	185.71	-38.76
35	3.62×10^{09}	137.88	186.51	-76.25
40	3.01×10^{10}	148.67	186.12	-58.72
45	4.51×10^{11}	162.49	185.66	-36.33
50	1.01×10^{10}	142.96	186.32	-67.98
55	1.42×10^{10}	144.68	186.25	-65.18
60	2.57×10^{12}	171.34	185.39	-22.02
65	1.67×10^{11}	157.25	185.83	-44.81
70	2.55×10^{12}	171.25	185.39	-22.17
75	5.10×10^{16}	222.11	184.04	59.70
80	1.79×10^{16}	216.13	184.17	50.13
Average		**156.19**	**185.97**	**-46.68**

Frequency factor which is often called as pre-exponential factor indicates the number of collisions happening among reactant molecules during thermal decomposition of biomass and it directly reflects the direct proportionality to the level of complexity in pyrolysis of biomass. The values of pre-exponential factor calculated from three iso-conversional models were found to be in the range of 2.78×10^5 - 4.99×10^{16}, 6.31×10^5 - 2.21×10^{16} and 2.94×10^5 - 5.10×10^{16} for KAS, FWO and Starink models respectively with conversion ranging from 10 to 80%. This wide range of pre-exponential factor along with increasing conversion of biomass indicates heterogeneous and complex properties of biomass besides complexities of multi-step reaction mechanism occurring while the decomposition of biomass takes place (EL-Sayed et al., 2021). Pre-exponential value less than 10^9 indicates surface reaction and attributes to the formation of a closed complex and easy degradation whereas a value more than 10^9 is due to the formation of a simple and loose complex (Maia et al., 2016; Ahmad et al., 2021). From Table 3.6, it is evident that pre-exponential factor values greater than 10^9 are obtained for almost entire range of conversion except for initial states only and thus signaling formation of a loose

and simpler complex, low rate of degradation and high energy requirements for decomposition. Also, pre- exponential factor and activation energy followed a directly proportional relationship, means with increase in the value of activation energy pre-exponential factor value also increased and with decrease in the value of activation energy pre-exponential factor value decreased, too. Furthermore, pre-exponential values reported in earlier studies for different feedstocks were like acacia nilotica (10^{10}–10^{25} s^{-1}) (Singh et al., 2020), maize cob (10^{5} –10^{23} s^{-1}) (Gupta and Mondal 2019b), Para grass (1.42×10^{7} –2.26×10^{19} s^{-1}) (Ahmad et al., 2017a).

An integral key parameter for thermodynamic assessment is change in enthalpy. Change in enthalpy indicates if energy is gained or lost by the system and also whether reaction is endothermic or exothermic in nature. The average values of change in enthalpy obtained for KAS, FWO and Starink iso-coversional models came out to be 155.91, 157.47 and 156.91 kJ/mol respectively. Here, since all ΔH values are positive and as we know that positive value of change in enthalpy indicates that the reaction is endothermic in nature, thus degradation of MAS into bio-oil, bio-char and gaseous products requires supplying energy in the form of heat from surroundings to the system. Beyond 65% conversion, ΔH increased significantly which indicates high energy is required for decomposition of MAS in this range as mainly lignin portion is left for degradation post hemicellulosic and cellulosic portion degradation. It was also noted that at any specific conversion over the entire range, difference between activation energy and change in enthalpy was around 5 kJ/mol for all three models. It suggests that possibly there is not any energy barrier which can inhibit the formation of the products. It is worth noting that the small difference in activation energy and change in enthalpy values (~5 kJ/mol) designate favorable circumstances for the generation of activated complex (Akyurek, 2019; Daugaard and Brown, 2003). ΔH values in this present study were less than that reported

in literate for *Typha latifolia* (177.51 kJ/mol) for FWO, *Typha latifolia* (179.42 kJ/mol) for KAS (Ahmad et al., 2017b), maize cob (180.58 kJ/mol) (Gupta and Mondal, 2019b) for KAS, ΔH values were more than that for maple leaf waste (85.16 kJ/mol) for FWO (Ahmad et al., 2021) and for red pepper waste(87.62 kJ/mol) for FWO (Maia et al., 2016). The change in Gibbs free energy (ΔG) represents the available energy from biomass which canbe utilized for formation of activated complex. The values of ΔG obtained for KAS, FWO and Starink models were 185.98, 185.91 and 185.97 kJ/mol respectively. A positive value of change in Gibbs free energy denotes that the reaction is non-spontaneous and thus demands external supply of energy. In recent reports ΔG values were reported as 160–200 kJ/mol for pinewood (He et al., 2019b), 171.64 kJ mol^{-1} for *Typha latifolia* (Ahmad et at., 2017b) and 154.3–400 kJ/mol for canola residue (Tahir et al., 2019). These findings revealed that MAS could be utilized as a potential bioenergy generating source.

Next thermodynamic parameter which was studied in this work was entropy. This property is used to indicate the randomness and disorder existing in any system. The values of ΔS obtained for KAS, FWO and Starink model were in the range varying from -154.18 to 59.41 J/mol.K, -147.27 to 52.76 J/mol.K, -153.62 to 59.70 J/mol.K respectively. High ΔS values indicate that material is far away from reaching its thermodynamic equilibrium while lower values of ΔS indicate that activated complex is having much organized structure as compared to the starting material and is at the brim of achieving thermal equilibrium and possessing considerable amount of heat energy supplied to it as unused or free (Yuan et al., 2017; Mishra et al., 2020). These all findings of this study related to both the positive and negative values of ΔS were yet another proof which emphasized that MAS is a potential biomass for exploration in the field of bioenergy generation.

3.3.6 Pyrolysis performance analysis

The values of T_p, T_i and $\Delta T_{1/2}$ increased as heating rate increased from 10 to 20 to 30 ℃/min as shown in Table 3.7. For maximum rate of decomposition, corresponding T_p value increased with elevation in rate of heating which could be attributed to the fact that mass and heat transfer rates of sample get affected and some sections of the resultant get no time for getting volatilized (Huang et al., 2018). Maximum and average decomposition rate values increased with enhancement in heating rate which indicated that pyrolysis performance is better at 30 ℃/min as compared to lower heating rates of 10 and 20 ℃/min. CPI values were calculated by using eq. 3.21 and came out to be 65.73, 176.63 and 210.76 for 10, 20 and 30 ℃/min, respectively. This increase in the value of CPI with increasing heating rate inferred that high heating rate condition outperformed the lower ones as higher values of CPI are indicator of better performance in terms of pyrolysis efficiency (Huanga et al., 2020). For various heating rates, pyrolysis performance efficiency is one of the operating key factors which we need to consider while scaling up to the industrial level. Here, in this case 30 ℃/min heating rate seemed to be a better option for carrying out pyrolysis of MAS as reflected by higher values of R_a, R_p and CPI.

Table 3.7. Pyrolysis performance parameters of MAS at different heating rates (β)

Parameters	**β**	**Value of parameter**
Maximum decomposition rate ($-R_p$, %/min)	10	11.77
	20	22.61
	30	33.06
Average decomposition rate ($-R_a$, %/min)	10	1.13
	20	2.16
	30	3.14
Weight loss (M_f, %)	10	96.02
	20	96.15
	30	85.19

DTG maximum peak temperature (T_p, ℃)	10	364.93
	20	375.06
	30	390.16
Initial devolatilization temperature (T_i, ℃)	10	130.5
	20	141.2
	30	151.9
Half-peak width temperature range ($\Delta T_{1/2}$, ℃)	10	40.8
	20	50.2
	30	70.8
Comprehensive pyrolysis index (CPI, $10^{-5}.\%^3.{}^oC^{-3}.min^{-2}$)	10	65.73
	20	176.63
	30	210.76

3.4 Future outlook

This study emphasizes the candidature of MAS to be used for extracting bioenergy from it through the process of pyrolysis. Simultaneously dual purpose of energy generation from waste and thus reducing the burden on conventional sources of energy as well as waste management could be accomplished. MAS can be converted into a source of energy by thermochemical process of pyrolysis. Pyrolysis is a thermochemical process which is carried out in inert atmosphere and in turn lignocellulosic biomass fragments and depolymerizes into valuable products comprising of liquid bio-oil, solid bio-char and pyrolytic gaseous products. Pyrolytic liquid is product of the prime concern in pyrolysis and it is a highly oxygenated complex blend of chemical compounds like aliphatic and aromatic hydrocarbons including alcohols, esters, phenols, ketones, aldehydes, furans and organic acids. Quantitative and qualitative characterization of pyrolysis products is indispensable for evaluation of desired properties needed for downstream production of bioenergy, biofuels and chemicals from it. However, the products and their properties are highly influenced by many factors like rate of reaction and circumstances, composition of biomass, size of particle, sweeping gas flow rate and temperature. Pyrolysis reaction temperature is most instrumental parameter among all

above mentioned parameters. Thus, all operating parameters need to be chosen wisely and findings of present study can help us in this decision making. This study confirmed the high portion of bio-oil than solid bio-char and pyrolytic non-condensable gaseous products by pyrolysis owing to the fact that cellulose and volatile content is high in MAS. These products of pyrolysis viz. liquid bio-oil, solid bio-char and pyrolytic gases can easily and fruitfully be employed in different applications. Bio-oil consists of hydrocarbons and can be utilized to blend with petroleum products or in the form of liquid fuel in combustors. Although, bio-oil contains oxygenated compounds in large quantity which is a limitation but further upgradation of bio-oil by catalytic pyrolysis by using zeolites, etc. as catalyst can be carried out and enhancing bio-oil properties comparable to petrol and can be used as a fuel for transportation or value-added chemical. Bio-char is highly porous and carbon-rich solid having enormously high surface area which can find wild applications in various areas. Bio-char can be used as a carbon sequestration agent. Bio-char can also be deployed for water purification where it can be used as an adsorbent because it possesses high surface area, porous structure and enhanced surface chemical properties and as an additive for amendment of soil as it is capable of turning a barren land into fertile one owing to the fact that bio-char is a highly carbon rich material. Apart from these applications there is scope of examining efficiency of bio-char towards real-time discharge of industries and possibilities of bio-char regeneration. Bio-char also finds its applicability to be used as a meso-porous activated carbon precursor. Pyrolytic gaseous product of pyrolysis can be employed for co-firing in furnaces and also as a fuel for boilers and combustion engines as it is predominantly rich in syn-gas. Pyrolytic gases can also be utilized in Fischer-Tropsh process for the production of liquid hydrocarbons by enriching these gases with carbon monoxide and hydrogen. In this way, all the products of pyrolysis are beneficial. The

entire idea of biomass pyrolysis is based on the theme of converting waste into wealth. Sawdust which is a waste can be converted into an asset by employing pyrolysis process for harnessing bioenergy from it. It is noteworthy that bioenergy and biofuel generation from waste biomass not only reduces liability on non-renewable sources of energy but also provides us with solution of waste management which is a threat to environment if not done properly.

3.5 Conclusions

Results of physicochemical characterizations confirmed high volatile matter, low moisture and ash content and high holocellulose (cellulose and hemicellulose) besides considerable amount of HHV (16.34 MJ/kg) in MAS. TG analysis was executed to elucidate the pyrolytic nature, thermal decomposition behavior, kinetics and thermodynamics of MAS at three different slow heating rates (10, 20 and 30 ℃/min) in temperature ranging from ambient temperature to 900 ℃. It was also found from TG studies that thermal decomposition of MAS is a complicated and multi-step process consisting of elimination of moisture and following that decomposition of hemicellulose, cellulose and lignin and finally formation of char. Maximum loss in mass was recorded in the temperature range of 210 to 480 ℃ indicating optimum range of temperature in which pyrolysis process can be performed. Multi-step kinetics was detected from KAS, FWO and Starink models which were employed in kinetics assessment and thus indicated the complex behavior of MAS pyrolysis signifying occurrence of many reactions simultaneously. Master-plot methodology along with Criado method was used for estimation of reaction mechanism which reflected different mechanisms of reaction governing different ranges of conversion of biomass. Initially, diffusion models like D2 and D3 were dominant and as conversion progressed first order random nucleation became controlling mechanism and as further conversion

proceeded contracting sphere and first, second and third order reaction models came into the mainstream. Thermodynamic study revealed high values of ΔG and low ΔH. Pyrolysis performance analysis showed higher CPI values at higher heating rate indicating better pyrolysis efficiency at high heating rate. All these findings recommended suitability of MAS for bioenergy generation as it exhibits remarkably high potential for bioenergy generation. Based on all these findings it can be inferred that MAS could yield a stellar performance for clean energy aspirations' actualization. Utilization of waste biomass into biofuel and bioenergy production is a pragmatic and resilient approach as it will open up new avenues of growth and help pertain the goal of achieving energy emancipation along with overcoming contemporary issues created by utilization of fossil fuels.